# Poled polymer thin-film gratings studied with far-field optical diffraction and second-harmonic near-field microscopy

**R. D. Schaller and R. J. Saykally**

*Department of Chemistry, University of California, Berkeley, Berkeley, California 94720-1460*

**Y. R. Shen and F. Lagugné-Labarthet**

*Department of Physics, University of California, Berkeley, Berkeley, California 94720*

Received March 26, 2003

Electrical poling induces polar ordering of molecules in a grating that has been holographically inscribed on a thin film of polymer with azobenzene side chains. The resulting $\chi^{(2)}$ grating, seen by second-harmonic-generation (SHG) near-field scanning optical microscopy, can have a periodic structure that is significantly different from the topographical image. The far-field linear and SHG diffraction patterns correlate well with the grating structures. Poling of the thin-film grating, which presumably has photodriven nonuniform material properties within each period, leads to the more complex structure of the $\chi^{(2)}$ grating. © 2003 Optical Society of America

*OCIS codes:* 230.1950, 240.4350, 230.4320, 180.5810, 190.4400.

Mesostructured materials with large optical nonlinearities have potential applications in photonics, such as Bragg filters, and in fiber-optic coupling.[1] $\chi^{(2)}$ nonlinear optical gratings are of special interest because they can generate diffracted second-harmonic (SH) beams that can be spatially separated from the input and diffracted fundamental waves.[2,3] Here we report second-harmonic-generation (SHG) studies of electrically poled surface-relief gratings (SRGs) that were holographically inscribed on amorphous polymer thin films functionalized with nonlinear optical chromophores. We show that such gratings can have a doubly peaked $\chi^{(2)}$ periodic structure compared with the geometric grating structure. Such a $\chi^{(2)}$ grating presumably results from poling of a SRG that has material structural variation from ridges to valleys created during photoprocessing.

The polymer thin films were spin coated onto glass slides from a solution (5% by weight) of poly(4′{[2(methacryloyoxy)ethyl]amino}4-nitroazobenzene) [p(DR1M); Ref. 4] in chloroform and had a thickness of 400 nm. The gratings were inscribed on the films by photoisomerization with two *p*-polarized, overlapping $Ar^+$ beams ($\lambda = 514.5$ nm) incident at an angle of ~11° from opposite sides of the surface normal, each with an intensity of 40 mW/cm$^2$.[5] Photoisomerization caused the polymeric material to flow out of the higher laser intensity region and yielded a geometrical grating structure that could be detected by atomic-force microscopy (AFM) [Fig. 1(a)]. The gratings had an area of 3 mm in diameter. They were electrically poled by a thin tungsten wire, situated 5 mm above the film, oriented perpendicular to the grating grooves, and biased at 3 kV [Fig. 1(a)]. After 1 h of poling at 90 °C, which is 30 °C below the glass transition temperature ($T_g$) of the material, the films were cooled to room temperature with the bias potential on. When it was applied to a flat p(DR1M) film, this poling procedure created a large second-order nonlinear optical coefficient, $d_{33} \sim 250$ pm/V, for the film that lasted for months without deterioration.

Two different gratings were fabricated on p(DR1M) films with different laser irradiation times and poled as described above. The gratings had the same periodicity of 1.4 $\mu$m but different surface-relief amplitudes of 100 and 400 nm, as determined by AFM. When each grating was probed by a normally incident He–Ne laser beam ($\lambda = 632.8$ nm), it yielded a linear diffraction pattern showing prominent first-order diffraction [Fig. 2(a)]. The diffraction efficiencies of the two gratings were 5% and 25%, respectively. Using a normally incident 1.064-$\mu$m laser beam with polarization perpendicular to the grating grooves [Fig. 1(b)], we also measured SH diffractions at 532 nm in transmission and found them to be *p* polarized. The gratings exhibited diffraction patterns with comparable first- and second-order diffraction peaks but no zeroth-order peak [Fig. 2(b)]. In particular, the 400-nm grating had stronger second- than

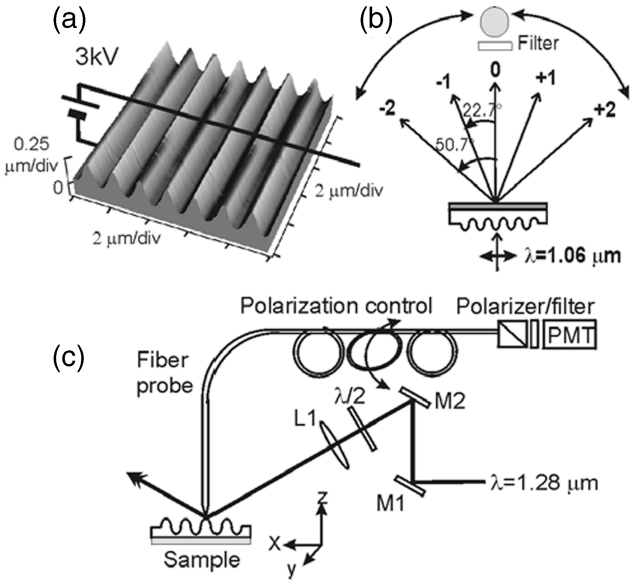


Fig. 1. (a) Poling schematic of the thin-film grating. Note that the vertical and horizontal length scales are different. (b) SHG diffraction setup. (c) NSOM setup.

0146-9592/03/151296-03$15.00/0 

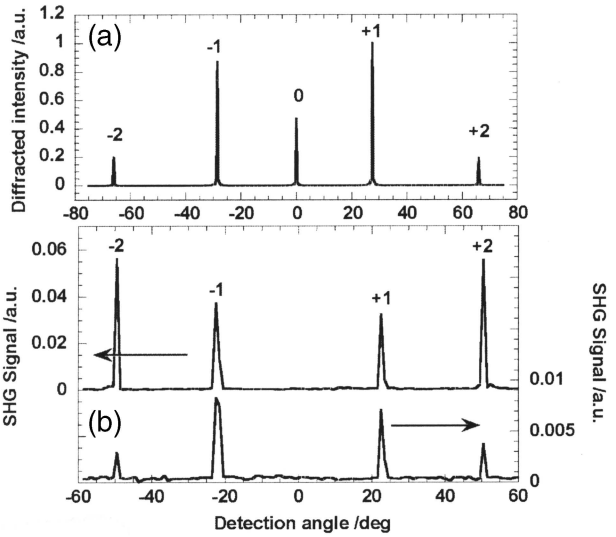


Fig. 2. (a) Far-field linear diffraction pattern for the 400-nm grating observed with a horizontally polarized He–Ne laser beam at $\lambda = 632.8$ nm. (b) Far-field SHG diffraction patterns for (top) 400-nm and (bottom) 100-nm gratings observed by an input Nd:YAG laser at $\lambda = 1064$ nm.

first-order diffraction. This result indicates that the $\chi^{(2)}$ grating structure is different from the linear (or geometric) grating structure. The measured first-order–second-order diffraction peak intensity ratio was 1.9 for the 100-nm grating and 0.66 for the 400-nm grating.

In our poling geometry, the poling field at the polymer surface was roughly along the grating surface normal, despite the appreciable periodic variation of the surface profile. We can therefore approximate the local $\overleftrightarrow{\chi}^{(2)}(x)$ by a uniaxial $C_{\infty v}$ symmetry, with $\hat{x}$ taken as perpendicular to the grating grooves. Then, the nonvanishing $\overleftrightarrow{\chi}^{(2)}(x)$ elements are $\chi^{(2)}_{zzz}$, $\chi^{(2)}_{zxx} = \chi^{(2)}_{zyy}$, and $\chi^{(2)}_{xzx} = \chi^{(2)}_{yzy} = \chi^{(2)}_{xxz} = \chi^{(2)}_{yyz}$, where $z$ is along the grating surface normal. For a normally incident fundamental input beam, one can obtain access to only the $\chi^{(2)}_{zxx} = \chi^{(2)}_{zyy}$ element. Therefore, no SHG in transmission along the surface normal is allowed. This explains why the zeroth-order SHG was not observed in transmission and the diffracted SH output was $p$ polarized. The diffracted beams were in the directions predicted by the law of diffraction.

One would suspect that poling might have created a $\chi^{(2)}$ grating with a periodic structure different from that of the linear or topographical grating. To probe the mesostructure of the $\chi^{(2)}$ grating, we employed second-harmonic generation near-field scanning optical microscopy (SHG NSOM). Measurements were carried out with a shear-force feedback NSOM apparatus in the collection mode, shown experimentally in Fig. 1(c).[6] An amplified femtosecond titanium:sapphire pulsed laser in conjunction with an optical parametric amplifier system generated 80-fs pulses at 1.28 $\mu$m with energy of 250 nJ/pulse, which were used as the fundamental input. The input beam was focused to a spot size of $(100\ \mu\text{m})^2$ on the sample beneath the NSOM probe, with an incidence angle of 60°. The incidence plane was perpendicular to the grating lines. The SHG photons collected in the near field were sent through proper filters and detected by a photomultiplier coupled with a gated integrator. The optical fiber used in the NSOM was a single-mode fiber, and the polarization was preserved over the fiber length (~80 cm). The observed cross-polarization extinction ratio at 532 nm was 30:1. Figure 3 displays simultaneously collected topographical and SHG NSOM images of the two gratings with $p$-polarized input. Although the shallower (100-nm) SRG shows, within noise, a periodically structured SHG NSOM image [Fig. 3(b)] similar to that of the topographical image [Fig. 3(a)], the deeper (400-nm) SRG [Fig. 3(c)] yields a SHG NSOM image [Fig. 3(d)] that exhibits double peaks at the ridges. In both cases, the corresponding linear NSOM image of the poled grating resembled that of the topographical image. Figure 4 quantifies the structure of the SHG NSOM images of the 400-nm grating (along a line perpendicular to the grating) obtained with the $P_{\text{in}}P_{\text{out}}$ and $S_{\text{in}}P_{\text{out}}$ polarization configurations. The unequal amplitudes of the double peaks in the images were caused by having the pump beam incident on the sample at a finite angle and can be corrected with appropriate Fresnel coefficients.

The $\chi^{(2)}$ grating structure should be related to the far-field SH diffraction pattern by Fourier transform (FT). Shown in the inset of Fig. 4 are the FTs of the SHG NSOM images of the 400-nm grating for the $P_{\text{in}}P_{\text{out}}$ and $S_{\text{in}}P_{\text{out}}$ polarization combinations. As expected, they reveal first- and second-order diffraction peaks of comparable strength. In particular, the $S_{\text{in}}P_{\text{out}}$ case should record the $\chi^{(2)}_{zyy}$ structure, and therefore its FT should be compared with the observed SHG diffraction pattern shown in Fig. 2(b) for the

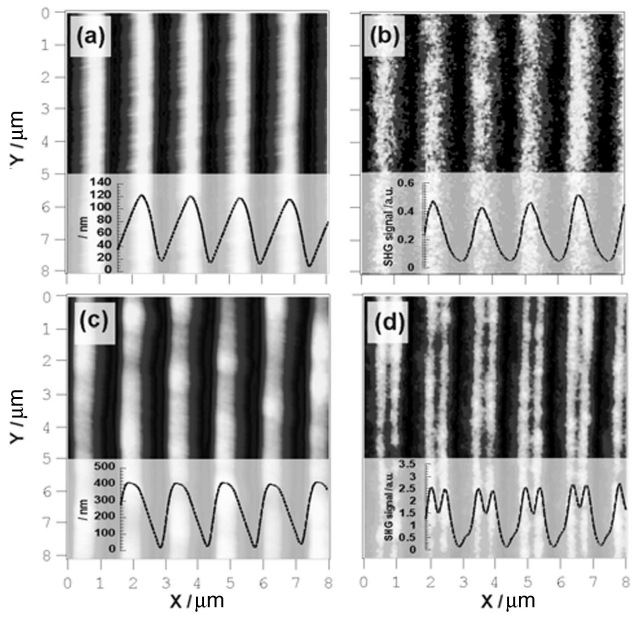


Fig. 3. (b), (d) SHG NSOM images for p(DR1M) thin-film gratings with grating amplitudes of 100 and 400 nm, respectively, obtained with 1.28-$\mu$m femtosecond input pulses. The corresponding topographical images are shown in (a) and (c).

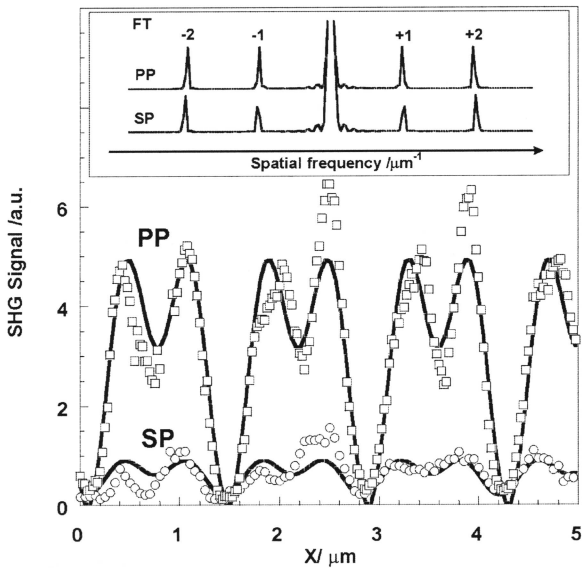


Fig. 4. Periodic variations of SHG NSOM in scans across the grating lines with $P_{in}P_{out}$ and $S_{in}P_{out}$ polarization combinations for the 400-nm grating. Experimental data points (open circles) after correction by Fresnel coefficients are approximated by the solid curves. FTs of the solid curves are displayed in the inset. The SHG profile for the $S_{in}P_{out}$ case should be compared with the SHG diffraction pattern from the same grating in Fig. 2(b).

400-nm grating. We note that the agreement between the two is very good. We have also quantified the SHG NSOM image of the 100-nm grating and found that its FT has a more dominant first-order diffraction peak and is in agreement with the far-field diffraction pattern presented in Fig. 2(b).

The double-peak periodic $\chi^{(2)}$ structure can be understood from the history of grating formation. The formation of SRGs on amorphous azopolymers is most efficient with interfering waves polarized perpendicular to the grating lines and is the result of photodriven mass transport from successive photoisomerization steps.[7,8] Such a photoinduced mechanism suggests possible strong alterations of local viscoelastic properties of the polymer. Studies using Raman microscopy[9] revealed that the local orientation of the azobenzene side chains is modified by transport of the polymeric material from the valleys to the ridges, and the density at the ridges appears significantly higher. In a copolymer containing 12% molar azochromophores in the side chain, the density increase was estimated to be 5%.[9] The increase is expected to be higher in homopolymer in which a stronger surface modulation has been observed. Thermal annealing could erase the grating structure; x-ray diffraction from such a film still exhibited a remnant periodic density variation.[10] AFM studies of these films showed that the nonirradiated part of the polymer film appeared stiffer than the irradiated part.[11] All these results, together with the observed topography of the grating, indicate that formation of the SRG is the consequence of photodriven transport of polymeric materials from the strong field region to the weak field region; the latter is more densely packed.

A higher density results in a higher glass transition temperature ($T_g$) of the polymer. At a given temperature, it is more difficult to electrically pole the part that has a higher $T_g$ and is mechanically stiffer. Thus one can expect that the ridges of the grating, which have a higher $T_g$, will be less effectively poled. The effect is more obvious on a deeper grating, causing the observed dips of SHG efficiency at the top of the ridges. The SH output from the valleys of the gratings was even weaker than that from the ridges. This weaker output is because the average thickness of the polar-ordered film that we used was comparable to the grating depth, and hence the true local film thickness contributing to the SHG was appreciably smaller in the valleys, yielding a weaker SH output.

In summary, the observed far-field SH diffraction patterns and SHG NSOM images obtained from a poled grating inscribed on a polymer film containing azobenzene are well correlated. For a grating of sufficient modulation depth, the $\chi^{(2)}$ periodic structure appears quite different from that the topography revealed by linear NSOM or AFM. Photoisomerization of the azobenzene side chains used to form the grating is known to result in mass transport and to make the mass density higher at the ridges than the valleys. Less-effective poling at regions with higher density could lead to the observed complex $\chi^{(2)}$ structure.

The work of Y. R. Shen and F. Lagugné-Labarthet was supported by the U.S. Department of Energy under contract DE-AC03-76SF00098. R. D. Schaller and R. J. Saykally are supported by National Science Foundation grant CHE-9727302. F. Lagugné-Labarthet's e-mail address is lagugne@socrates.berkeley.edu.

## References

1. Y. Che, O. Sugihara, C. Egami, H. Fujimura, Y. Kawata, N. Okamoto, M. Tsuchimori, and O. Watanabe, Jpn. J. Appl. Phys. **38,** 6316 (1999).
2. G. Martin, E. Toussaere, L. Soulier, and J. Zyss, Synth. Met. **127,** 49 (2002).
3. L. M. Blinov, S. P. Palto, S. G. Yudin, M. P. De Santo, G. Cipparone, A. Mazzulla, and R. Barberi, Appl. Phys. Lett. **80,** 16 (2002).
4. S. Xie, A. Natansohn, and P. Rochon, Macromolecules **27,** 1885 (1995).
5. F. Lagugné-Labarthet, T. Buffeteau, and C. Sourisseau, Appl. Phys. B **74,** 129 (2002).
6. R. D. Schaller, J. C. Johnson, K. R. Wilson, L. F. Lee, L. H. Haber, and R. J. Saykally, J. Phys. Chem. B **106,** 5143 (2002).
7. P. Lefin, C. Fiorini, and J. M. Nunzi, Pure Appl. Opt. **7,** 72 (1998).
8. N. K. Viswanatahan, S. Balasubramanian, L. Li, S. K. Tripathy, and J. Kumar, Jpn. J. Appl. Phys. **38,** 5928 (1999).
9. F. Lagugné-Labarthet, T. Buffeteau, and C. Sourisseau, Macromol. Symp. **137,** 5 (1999).
10. T. M. Geue, M. G. Saphiannikova, O. Henneberg, U. Pietsch, P. L. Rochon, and A. L. Natansohn, Phys. Rev. E **65,** 052801 (2002).
11. T. Ikawa, T. Mitsuoka, M. Hasegawa, M. Tsuchimori, O. Watanabe, Y. Kawata, C. Egami, O. Sugihara, and N. Okamoto, J. Phys. Chem. **104,** 9055 (2000).